Institute for Software Integrated Systems
Vanderbilt University
Nashville, Tennessee, 37235

A Backstepping Control Framework for m-Triangular Systems

Nicholas Kottenstette, Heath LeBlanc, Emeka Eyisi, Joseph Porter

TECHNICAL REPORT

ISIS-11-104

Original Draft: 03/15/2011
Revised Draft: 04/01/2011
Official Release: 04/28/2011
NOTICE: A slightly different version of this technical report is currently under review in the IEEE Transactions on Control Systems Technology under the following title, “A Backstepping Control Framework for Networked Control of m-Triangular Systems”, Nicholas Kottenstette, Heath LeBlanc, Emeka Eyisi, Joseph Porter.

***Abstract*— m-Triangular Systems are dynamical physical systems which can be described by m triangular subsystem models. Many physical system models such as those which describe fixed-wing and quadrotor aircraft can be realized as m-Triangular Systems. However, many control engineers try to fit their dynamical model into a 1-Triangular System model. This is commonly seen in the backstepping control community in which they have developed pioneering adaptive control laws which can explicitly account for operating state constraints. We shall demonstrate that such control laws can even be implemented in a non-adaptive form while still addressing actuator limitations such as saturation. However, most importantly, by removing the adaptation component, a *strictly output passive* input-output mapping can be realized. This important property is most applicable to the networked control community. For the networked control community, this *key property* allows us to integrate an aircraft into our framework such that a *discrete-time lag compensator* can be used by a ground control station for remote navigation in a *safe and stable manner in spite of time-varying delays and random data loss*. The applicability of our result shall be made clear as we demonstrate how an inertial navigation system for a quadrotor aircraft can be constructed. Specifically: i) the desired inertial position ($\zeta_s = [\zeta_{Ns}, \zeta_{Es}, \zeta_{Ds}]^\mathsf{T}$) and yaw ($\psi_s$) setpoints can be concatenated to consist of the *virtual* desired setpoint ($\bar{u} = [\zeta_s^\mathsf{T}, \psi_s]^\mathsf{T}$); ii) the *virtual* desired setpoint corresponds to the $m = 3$-concatenated state outputs $\bar{x} = [x_{(1,1)}^\mathsf{T}, x_{(2,1)}^\mathsf{T}, x_{(3,1)}^\mathsf{T}]^\mathsf{T} = [[\zeta_N, \zeta_E], \zeta_D, \psi]^\mathsf{T}$; which iii) are augmented such that the output $\bar{v}$ equals $\bar{x}$ at steady-state operation; iv) using Lemma 1 we can show that the backstepping framework renders the quadrotor aircraft to be strictly output passive (sop) ($\dot{V}(v) \leq -\epsilon_b \bar{v}^\mathsf{T}\bar{v} + \bar{v}^\mathsf{T}\bar{u}$) such that $V(v) = \frac{1}{2}v^\mathsf{T}v$ is a Lyapunov function in terms of all concatenated system states v associated with the m-Triangular System. Lemma 2 then shows how the resulting continuous-time strictly output passive system involving the quadrotor aircraft can be integrated into an advanced digital control framework such that a strictly output passive *discrete-time lag* compensator can be used to control the inertial position from a ground-station in an L_2^m-stable manner such that time-delays and data loss will not cause instabilities.**

I. Prologue

This technical note concludes a chapter in my early research career. In particular it presents a general framework to allow an engineer to interconnect m-Triangular Systems to a discrete-time lag controller in a safe and stable manner in spite of arbitrary sampling rates T_s and communication delays between the digital controller and a m-Triangular System. I had set out to develop such a framework approximately ten years ago while working as a member of the Advanced Technology Group at MKS Instruments. At MKS I helped develop an ethernet enabled pressure insensitive mass flow controller known as the πMFC (piMFC) [1]. The piMFC is an advanced cyber-physical system (CPS) in which each member of the development team inherently understood how the entire CPS functioned; however, each member had depth within a given discipline in order to address specific aspects of that CPS.

At the time, my depth was in advanced digital control software development, analog sensor, actuator and embedded systems design. Many of the digital MFCs developed during this time were required to be interconnected to a low-bandwidth controller area network (CAN) interface and comply with a high-level specification known as DeviceNet [2]. I had witnessed that the product engineers were struggling to get their products to comply with an overly complex and demanding timing specification. Why would there be such demanding real-time constraints on a high-level communications protocol in which most of the real-time control functions were delegated to advanced devices such as the piMFC? My assertion at the time was that many of the large system integrators i) did not fully understand where delays were being introduced into their systems; and ii) could not precisely determine how a given amount of communication delay would affect system stability. As a result the large system integrators were unable to determine the correct communication and subsystem specifications in order to reduce the costs for advanced subsystem components such as the piMFC.

For example, the reason I insisted that the piMFC electronics should have an ethernet interface is that I wanted to demonstrate to the large system integrators that there were better, less expensive high-bandwidth communication alternatives then the costly and overly complicated DeviceNet connectors and their corresponding specifications. The resulting benefits of this choice were obvious, we were able to easily provide a web-enabled diagnostic interface while being able to quickly adapt the system to fit the customers needs.

At the University of Notre Dame I honed my skills as a mathematician in order tackle this challenging problem. In order to address this problem I looked to the telemanipulation community which had to cope with time-delay [3], [4]. I had a strong bias for the work of [4] because it was explained in a physically and graphically intuitive manner which resonated with my mechanical engineering expertise, whose skills I mastered at MIT under the direction of Professor Woodie Flowers. These aforementioned works presented an architecture in which continuous-time robotic systems and their corresponding continuous-time controllers were interconnected in a *passivity* preserving manner through the use of *wave variables*. The wave variables allowed the system to tolerate arbitrary fixed-time delay while preserving system-stability in which initial efforts to handle time-varying delays are discussed in [4].

The general approach was to send and receive continous-time wave variables in a manner such that the continuous-time L_2^m-norm of the received input waves will remain bounded by the corresponding L_2^m-norm of the sent output waves in order to maintain an overall passive system architecture. The following passivity preserving property holds in general when wave variables are subject to fixed-delays; however, for time varying delays careful processing of the received input waves is required. As a result of applying this approach, novel compression and decompression algorithms emerged as discussed in [5]–[7]. However, our primary concern was to develop a framework which *explicitly* allowed for digital controllers to be interconnected to non-linear continuous-time systems.

0

Contract/grant sponsor (number): NSF (NSF-CNS-1035655)
Contract/grant sponsor (number): Air Force (FA9550-06-1-0312)

Therefore, we initially evaluated a similar *lossy data reduction* algorithm as compared to the Compressor/Expander formulation presented in [5] for the discrete-time case as discussed in [8, Section 4.3.1] which ultimately was not suitable for our architecture as it introduced significant *distortion* in our system response. We found that a much more effective approach was to execute our controller in an *asynchronous* manner which was triggered by the arrival of discrete wave variable data from the plant. The overall flow of controller execution was precisely governed by a *Passive Asynchronous Transfer Unit* [9]. The framework presented in [9]; contained a causal passivity preserving set of elements we refer to as the *inner-product equivalent sample and hold* (IPESH).

The IPESH is based on the pioneering work of [10] whose approach was adopted by [11] and others. A *sampler and zero-order hold* was presented in a framework which allows an engineer to interface continuous-time Port Controlled Hamiltonian Systems (PCHSs) to discrete-time Port Controlled Hamiltonian Systems. PCHSs are a class of *passive systems* which provide a relatively general framework to describe system models whose relationships are governed by a Dirac structure [12] and are used extensively to model robotic systems [13]. The PCHSs framework is a generalized version of the bond-graph formulation pioneered by Henry Paynter [14] in which the *effort* and *flow* components were treated as scalars and interconnections were constrained to a Dirac structure in order to describe a system model.

Although PCHs models are quite powerful to describe a system model, they are a bit difficult to use in a general control framework. For example a system model can be described in a graphical form without ever having to denote the systems inputs or outputs nor is it necessary to formulate a causal system description until later on in the design process [15]. Therefore we initially chose to present their *sampler and zero-order hold* in a *causal manner* in which we chose to refer to it as the IPESH [16, Definition 4] while *correcting an apparent typo* in the presentation of [10, Thorem 1] in which it appears the equation should have read $f_d(k+1) = q(kT) - q((k+1)T)$.

Our causal IPESH definition allowed us to connect the work of [17], [18] to the work of [10] in which they proposed a discrete-time (DT) passivity preserving observer structure for continuous-time (CT) linear time-invariant (LTI) systems. The resulting observer structure proposed in [17] is a direct result of applying the IPESH and the preservation of passivity is a direct result of [16, Theorem 3-I]. The proof provided in [17] was based on a dissipative systems theory approach and was extremely involved, we refer the reader to [19, Appendix E] for additional details.

One advantage of the causal IPESH formulation is that we could show that the LTI observers [20, Theorem 7] not only preserved passivity but stronger forms of passivity including *strictly input passive* and *strictly output passive* relationships [16], [21]. These results allowed us to eventually show that for the more general case, the *interior conic* properties [22], [23] are preserved after the IPESH is applied to a continuous-time interior conic system in order to derive a discrete-time input-output mapping [24, Lemma 3]. Similar properties can be found when applying the *bilinear-transform* [25] to a continuous-time filter in order to derive a discrete-time filter; however, the resulting discrete-time filters derived from the IPESH appear to *warp less* in their frequency response as clearly demonstrated by the bandpass filters derived using the *IPESH-Transform* [19, Definition 5].

The IPESH can be realized with an observer in order to connect a continuous-time LTI systems to a discrete-time controller. However, it is extremely challenging to implement an observer in order to *precisely* satisfy the IPESH for a non-linear system. The majority of these connections were primarily being made while I was at the University of Notre Dame. However, I was invited to apply these techniques at the Institute for Software Integrated Systems (ISIS) to a non-linear robotic system, quadrotor aircraft and fixed-wing aircraft. At ISIS I was part of an advanced CPS research team of engineers including Heath LeBlanc, Emeka Eyisi, and Joseph Porter. Our combined research efforts allowed us to develop five key works with others at ISIS which were instrumental in allowing us to present the following result [19], [24], [26]–[28].

II. Introduction

In this paper, we generalize the triangular system formulation – which is amenable to backstepping control techniques – by introducing the notion of m-triangular systems. We then show how a general backstepping controller can be integrated into the m-triangular system model. Our formulation of the backstepping control architecture enables us to prove that the augmented system is strictly output passive. This important property allows for the backstepping control architecture to be integrated into the networked control architecture given in [24]. This framework is applicable to the control of many classes of systems, including robotic systems [5], ground vehicles [29] and certain classes of chemical processes [30]–[32]. We illustrate how the backstepping control architecture can be applied in practice by demonstrating how to formulate the problem on a quadrotor aerial vehicle [27]. Finally, we show how to incorporate the backstepping control framework into our networked control architecture through simulations of a model of the Hummingbird quadrotor [33], [34].

The paper is organized as follows. Section IV introduces the m-triangular system model, while Section V describes the backstepping control framework for m-triangular systems. We analyze the strictly output passive input-output mapping resulting from the backstepping control architecture in Section VI. We recall the quadrotor model from [27] in Section VII, and then illustrate how to model it as a 3-triangular system in Section VIII. The networked control architecture from [24] is described in Section IX, along with results proving that the overall closed-loop system is strictly output passive and L_2^m-stable [26]. Simulations of a quadrotor model are given in Section X. Finally, conclusions are stated in Section XI.

III. Preliminaries

As presented in [24] and inspired by [22], [23], [35] we shall consider the following class of causal non-linear finite-dimensional continuous-time (discrete-time) systems $H : u \to y$ which are affine in control:

$$\dot{x}(t) = f(x(t)) + G(x(t))u(t),\ x(0) = x_0 = 0,\ t \geq 0 \quad (1)$$
$$y(t) = h(x(t)) + J(x(t))u(t)$$

for the continuous-time case in which the functions indicated in (1) are sufficiently smooth to make the system well defined [36], and

$$x(j+1) = f(x(j)) + G(x(j))u(j),\ x(0) = x_0 = 0 \quad (2)$$
$$y(j) = h(x(j)) + J(x(j))u(j)$$

for the discrete time case ($j = \{0, 1, \dots\}$) in which $x \in \mathbb{R}^n$, $u, y \in \mathbb{R}^m$ in which n and m are positive integers. We shall consider the following interior conic-dissipative supply function $s(u, y)$ as it relates to conic-dissipative systems which are inside the sector $[a, b]$ ($a < b$) [37]–[39]:

$$s(u,y) = \begin{cases} -y^{\mathsf{T}}y + (a+b)y^{\mathsf{T}}u - abu^{\mathsf{T}}u, & |a|,|b| < \infty \\ y^{\mathsf{T}}u - au^{\mathsf{T}}u, & |a| < \infty,\ b = \infty. \end{cases} \quad (3)$$

Definition 1: The continuous-time system $H : u \to y$, $x_0 = x(0) = 0$ whose dynamics are determined by (1) is a continuous-conic-dissipative system inside the sector $[a, b]$ with respect to the supply (3) if:

$$\int_0^T s(u,y)dt \geq 0,\ \forall T \ \geq 0. \quad (4)$$

Analogously the discrete-time system $H : u \to y$, $x_0 = x(0) = 0$ whose dynamics are determined by (2) is a discrete-conic-dissipative system inside the sector $[a, b]$ with respect to the supply (3) if:

$$\sum_{j=0}^{N-1} s(u,y) \geq 0,\ \forall N \ \in \ \{1, 2, \dots\}. \quad (5)$$

NB. the smoothness condition required by [36] appears to limit the discussion to systems which have finite-state-space descriptions and the resulting control system we will examine will be subject to time-delays which result in an infinite state-space. Therefore, if functions indicated in (1) are *not* sufficiently smooth but (4) is satisfied then the system $H : u \to y$ is a *continuous-conic system* inside the sector $[a, b]$. Finally the following notation will be used in order to represent time integrals, sums and norms:

$$\langle y, u\rangle_T = \int_0^T y^{\mathsf{T}}(t)u(t)dt$$
$$\|(y)_T\|_2^2 = \langle y, y\rangle_T,\ T \in \mathbb{R} \geq 0$$
$$\|y(t)\|_2^2 = \lim_{T\to\infty} \|(y)_T\|_2^2$$
$$\langle y, u\rangle_N = \sum_{j=0}^{N-1} y^{\mathsf{T}}(j)u(j)$$
$$\|(y)_N\|_2^2 = \langle y, y\rangle_N,\ N \in \{1, 2, \dots\}$$
$$\|y(j)\|_2^2 = \lim_{N\to\infty} \|(y)_N\|_2^2.$$

If the continuous-time or discrete-time two-norm can be distinguished from the discussion we will simply use the $\|y\|_2^2$ nomenclature.

From [36], [39] in regards to Lyapunov stability and from [22], [23], [40] in regards to L_2^m (l_2^m) stability conic-dissipative systems have the following important properties:

Property 1: There exists a storage function $V(x) \geq 0$ $\forall x \neq 0$, $V(0) = 0$ such that:

$$\dot{V}(x) \leq s(u,y)$$

for a continuous-conic-dissipative system and

$$V(x(j+1)) - V(x(j)) \leq s(u(j), y(j))$$

for a discrete-time-conic-dissipative system. If in addition $h(x_0) = J(x)0 = 0$ and $h(x) \neq 0$ when $x \neq 0$ so that $H : u \to y$ is zero-state detectable then $V(x) > 0\ \forall x \neq 0$. Therefore if $H : u \to y$ is inside the sector $[a, b]$:

i) and zero-state detectable and $|a| < \infty$, $b = \infty$ it is Lyapunov stable.
ii) and zero-state detectable and $|a|, |b| < \infty$ it is asymptotically stable.
iii) and $|a|, |b| < \infty$ then it is inside the sector $[-\gamma, \gamma]$ in which $\gamma = \max\{|a|, |b|\}$. Therefore, it is $L_2^m(l_2^m)$-stable in which:
$$\|y\|_2 \leq \gamma\|u\|_2. \quad (6)$$
iv) and $k \geq 0$ then kH is inside the sector $[ka, kb]$; $-kH$ is inside the sector $[-kb, -ka]$.
v) (Sum Rule) if in addition $H_1 : u_1 \to y_1$ is inside the sector $[a_1, b_1]$ then $(H + H_1) : u \to (y + y_1)$ is inside the sector $[a + a_1, b + b_1]$.

Therefore it is a simple exercise to show that a conic dissipative system which is inside the sector $[0, b]$ is also a *strictly output passive* system with storage function $V(x) \geq 0\ \forall x \neq 0$, $V(0) = 0$ such that:

$$\dot{V}(x) \leq -\epsilon_b y^{\mathsf{T}}y + y^{\mathsf{T}}u \quad (7)$$

in which $\epsilon_b = \frac{1}{b}$. In Section IV we shall proceed to present a new class of causal non-linear finite-dimensional continuous-time systems which are affine in control input as described by (1). We refer to these systems as m-Triangular Systems. Two important properties of this *new class* of systems is i) they allow us to *accurately describe* complex non-linear systems such as quadrotor aircraft, fixed-wing aircraft and ground vehicles, ii) allow us to present an advanced backstepping control framework to derive a *strictly output passive* mapping in order to integrate into our digital control architecture.

IV. m-Triangular Systems

An m-triangular system is a dynamic model comprised of m 1-triangular subsystems. The subsystems are allowed to be coupled together by a concatenated state vector x, which consists of all of the 1-triangular system states $x_{(j,i)}$, in which $j \in \{1, \dots, m\}$ and $i \in \{1, \dots, n_j\}$. Additionally, each system has a given actuator input term $u_j \in \mathbb{R}^{m_j}$, $m_j \in \mathbb{N}$. It is a more generalized model than that considered in [41], which considers a 1-triangular system ($j = 1$). Precisely, the system is described by $\sum_{j=1}^{m} n_j$ differential equations of the following form:

$$\dot{x}_{(j,i)} = f_{(j,i)}(x) + g_{(j,i)}(x)x_{(j,i+1)}$$
$$\dot{x}_{(j,n_j)} = f_{(j,n_j)}(x) + g_{(j,n_j)}(x)u_j,$$

where $x_{(j,i)} \in \mathbb{R}^{n_{(j,i)}}$, $n_{(j,i)} \in \mathbb{N}$, are the state vectors, $f_{(j,i)}(x) = f_{(j,i)} \in \mathbb{R}^{n_{(j,i)}}$ are x-dependent vector functions, and it is assumed that $g_{(j,i)}(x) = g_{(j,i)} \in \mathbb{R}^{n_{(j,i)} \times n_{(j,i+1)}}$ ($n_{(j,i)} \leq n_{(j,i+1)}$) are x-dependent, full row rank matrices, in which $n_{(j,n_j+1)} = m_j$. In the sequel, the matrix $g^{-1}_{(j,i)}$ denotes the right inverse of $g_{(j,i)}(x)$.

V. Backstepping Control Framework

The overall goal of our control architecture will be to derive a strictly output passive mapping between the *virtual desired* input $\bar{u}_{(j,1)} \in \mathbb{R}^{n_{(j,1)}}$ and an augmented output $v_{(j,1)}$, which includes $x_{(j,1)}$. This can be accomplished by choosing the *virtual control* inputs, $\alpha_{(j,i)}$, as follows:

$$\alpha_{(j,1)} = g^{-1}_{(j,1)} \left[\dot{x}_{(j,1),c} - k_{(j,1)}\tilde{x}_{(j,1)} - f_{(j,1)} + \bar{u}_{(j,1)} \right],$$
$$\alpha_{(j,i)} = g^{-1}_{(j,i)} \left[\dot{x}_{(j,i),c} - k_{(j,i)}\tilde{x}_{(j,i)} - f_{(j,i)} - g^{\mathsf{T}}_{(j,i-1)} v_{(j,i-1)} \right],$$
$$u_j = \alpha_{(j,n_j)}.$$

The filtered control reference and its corresponding derivative are denoted $x_{(j,i),c}$ and $\dot{x}_{(j,i),c} \in \mathbb{R}^{n_{(j,i)}}$, respectively. In addition, the feedback error is denoted $\tilde{x}_{(j,i)} = x_{(j,i)} - x_{(j,i),c}$, which is multiplied by the symmetric positive-definite matrix $k_{(j,i)} > 0$. The filtered control references are computed as follows ($x_{(j,1),c} = \dot{x}_{(j,1),c} = 0$):

$$\dot{q}_{1(j,i)} = q_{2(j,i)},$$
$$\dot{q}_{2(j,i)} = a_{ji} \left[S^R_{(j,i)} \left(b_{ji} \left[S^M_{(j,i)}(\alpha_{(j,i)}) - q_{1(j,i)} \right] \right) - q_{2(j,i)} \right],$$
$$x_{(j,i+1),c} = q_{1(j,i)},$$
$$\dot{x}_{(j,i+1),c} = q_{2(j,i)}, \quad \text{where } i \in \{1, \ldots, n_j - 1\},$$

in which $a_{ji} = 2\zeta_{(j,i)}\omega_{n(j,i)}$ and $b_{ji} = \frac{\omega_{n(j,i)}}{2\zeta_{(j,i)}}$, where $\omega_{n(j,i)}$ and $\zeta_{(j,i)}$ are positive real coefficients ($\zeta_{(j,i)} \in (0, 1]$). In addition, $S^M_{(j,i)}(\cdot)$ and $S^R_{(j,i)}(\cdot)$ are the respective controller state reference magnitude and rate limiters, such that for $l \in \{1, \ldots, n_{(j,(i+1))}\}$:

$$S^M_{(j,i)}(\alpha_{(j,i)})_l = \begin{cases} x^L_{(j,i+1)l} & \text{if } \alpha_{(j,i)l} < x^L_{(j,i+1)_l}, \\ x^U_{(j,i+1)l} & \text{if } \alpha_{(j,i)l} > x^U_{(j,i+1)l}, \\ \alpha_{(j,i)-l} & \text{otherwise} \end{cases}$$

and

$$S^R_{(j,i)}(\dot{\alpha}_{(j,i)})_l = \begin{cases} \dot{x}^L_{(j,i+1)l} & \text{if } \dot{\alpha}_{(j,i)l} < \dot{x}^L_{(j,i+1)l}, \\ \dot{x}^U_{(j,i+1)l} & \text{if } \dot{\alpha}_{(j,i)l} > \dot{x}^U_{(j,i+1)l}, \\ \dot{\alpha}_{(j,i)l} & \text{otherwise.} \end{cases}$$

The limits $x^L_{(j,i+1)l}$ ($\dot{x}^L_{(j,i+1)l}$) and $x^U_{(j,i+1)l}$ ($\dot{x}^U_{(j,i+1)l}$) are constants corresponding to the desired lower and upper operating magnitude and rate limits, respectively, and are associated with the l^{th} component of each subsystem's state vector $x_{(j,i+1)}$. The block diagram illustrating the computation of $x_{(j,i+1),c}$ and $\dot{x}_{(j,i+1),c}$ is shown in Fig. 1.

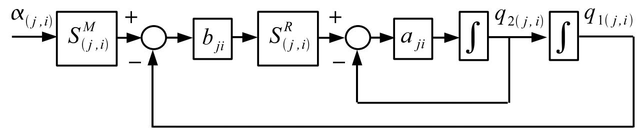

Fig. 1. Computation of $x_{(j,i+1),c}$ and $\dot{x}_{(j,i+1),c}$.

Finally, we define the augmented output as $v_{(j,i)} = \tilde{x}_{(j,i)} - \xi_{(j,i)}$. The term $\xi_{(j,i)}$ is computed as follows ($\xi_{(j,n_j)} = \dot{\xi}_{(j,n_j)} = 0$, $i \in \{1, \ldots, (n_j - 1)\}$):

$$\dot{\xi}_{(j,i)} = g_{(j,i)} \left[(x_{(j,i+1),c} - \alpha_{(j,i)}) + \xi_{(j,i+1)} \right] - k_{(j,i)}\xi_{(j,i)}.$$

It is obvious that our proposed formulation differs from that proposed by [41] in that we consider a novel m-triangular system formulation. However, there are small yet significant differences in our formulation that allow us to prove in Section VI that our proposed framework creates a strictly output passive mapping between the controller input $\bar{u} = [\bar{u}^{\mathsf{T}}_{(1,1)}, \ldots, \bar{u}^{\mathsf{T}}_{(m,1)}]^{\mathsf{T}}$ and an augmented output $\bar{v} = [v^{\mathsf{T}}_{(1,1)}, \ldots, v^{\mathsf{T}}_{(m,1)}]^{\mathsf{T}}$. The choice to include the vector $\bar{u}$ into our formulation is inspired by the earlier work presented in [42], which included a real term η_s in order to improve robustness for a given adaptive backstepping control law. In [42] if the adaptive approximation error $\bar{\epsilon}_s = 0$, then a strictly output mapping between an augmented scalar state variable $\bar{x}_s$ and input robustness term η_s would result.

Finally, the overall control structure involving the virtual control signals $\alpha_{(j,i)}$ and augmented terms $v_{(j,i)}$ mirrors the formulation presented in [43], except that we i) consider the rate and magnitude limitation functions included in the trajectory filters presented in [41], ii) include the strictly output passive term $\bar{u}$, and iii) derive the strictly output passive mapping between $\bar{v}$ and $\bar{u}$ such that if $\dot{\xi}_{(j,1)} = \xi_{(j,2)} = 0$, and $(x_{(j,2),c} - \alpha_{(j,1)}) = 0$ then $\bar{v} = \bar{x} = [x^{\mathsf{T}}_{(1,1)}, \ldots, x^{\mathsf{T}}_{(m,1)}]^{\mathsf{T}}$. As will be presented in Section VII the inertial position with respect to the North-East-Down reference frame for a quadrotor aircraft is denoted $\zeta = [\zeta_N, \zeta_E, \zeta_D]^{\mathsf{T}}$ in addition its corresponding yaw is denoted as ψ. *Property iii) is therefore important as it allows us to relate inertial and attitude set points* $\bar{u} = [\zeta_{Ns}, \zeta_{Es}, \zeta_{Ds}, \psi_s]^{\mathsf{T}}$ *to their corresponding outputs* $\bar{x} = [\zeta_N, \zeta_E, \zeta_D, \psi]^{\mathsf{T}}$ *when the desired control references and virtual control parameters are equal.*

VI. Backstepping Control Analysis

The proof required to derive a strictly output mapping between the input $\bar{u}$ and output $\bar{v}$ follows in a similar manner as that given for: i) [43, Theorem 1], which considered a scalar 1-triangular system, in that we chose a similar Lyapunov function; and ii) [28, Theorem 1], in that we take advantage of the resulting skew-symmetric property that results from the feedback terms involving $\xi_{(j,i)}$. We noticed these skew-symmetric structures arising from these backstepping control laws for adaptive controllers presented in [41], which relied on a recursive argument for their proofs.

In stating the following result, we use the compact notation to describe the vector v such that $v_{(j,)} = [v_{(j,1)}^{\mathsf{T}}, \ldots, v_{(j,n_j)}^{\mathsf{T}}]^{\mathsf{T}}$ and $v = [v_{(1,)}^{\mathsf{T}}, \ldots, v_{(m,)}^{\mathsf{T}}]^{\mathsf{T}}$.

Lemma 1: The continuous-time system considered in Section IV subject to the backstepping control framework presented in Section V results in a strictly output passive system with input $\bar{u}$ and output $\bar{v}$. Specifically, the following Lyapunov function, $V(v) = \frac{1}{2}v^{\mathsf{T}}v$, satisfies $\dot{V}(v) \le -\epsilon_b \bar{v}^{\mathsf{T}}\bar{v} + \bar{v}^{\mathsf{T}}\bar{u}$, in which $\epsilon_b = \lambda_{\min}(\operatorname{diag}\{k_{(1,1)}, \ldots, k_{(m,1)}\})$ is a positive real number resulting from the minimum eigenvalue of the diagonalized block matrix consisting of the feedback matrices $k_{(j,1)}$, $j = 1, \ldots, m$.

Proof: First we take the expression for the virtual control inputs $\alpha_{(j,i)}$ and solve for $\dot{x}_{(j,i),c}$ such that

$$\begin{aligned}
\dot{x}_{(j,1),c} =& g_{(j,1)}\alpha_{(j,1)} + k_{(j,1)}\tilde{x}_{(j,1)} + f_{(j,1)} - \bar{u}_{(j,1)} \\
\dot{x}_{(j,i),c} =& g_{(j,i)}\alpha_{(j,i)} + k_{(j,i)}\tilde{x}_{(j,i)} + f_{(j,i)} + g_{(j,i-1)}^{\mathsf{T}} v_{(j,i-1)}.
\end{aligned}$$

Subtracting the above expressions from the dynamic equations for the subsystems, in order to obtain $\dot{\tilde{x}}$, yields

$$\begin{aligned}
\dot{\tilde{x}}_{(j,1)} =& g_{(j,1)}\left(\tilde{x}_{(j,2)} + x_{(j,2),c} - \alpha_{(j,1)}\right) - k_{(j,1)}\tilde{x}_{(j,1)} + \bar{u}_{(j,1)} \\
\dot{\tilde{x}}_{(j,i)} =& g_{(j,i)}\left(\tilde{x}_{(j,i+1)} + x_{(j,i+1),c} - \alpha_{(j,i)}\right) \\
& - k_{(j,i)}\tilde{x}_{(j,i)} - g_{(j,i-1)}^{\mathsf{T}} v_{(j,i-1)} \\
\dot{\tilde{x}}_{(j,n_j)} =& - k_{(j,n_j)}\tilde{x}_{(j,n_j)} - g_{(j,n_j-1)}^{\mathsf{T}} v_{(j,n_j-1)}.
\end{aligned}$$

The final equation is a result of direct substitution of $u_j = \alpha_{(j,n_j)}$. Next, we take the above set of expressions and solve for $\dot{v}_{(j,i)} = \dot{\tilde{x}}_{(j,i)} - \dot{\xi}_{(j,i)}$ such that

$$\begin{aligned}
\dot{v}_{(j,1)} &= -k_{(j,1)}v_{(j,1)} + g_{(j,1)}v_{(j,2)} + \bar{u}_{(j,1)} \\
\dot{v}_{(j,i)} &= -k_{(j,i)}v_{(j,i)} - g_{(j,i-1)}^{\mathsf{T}} v_{(j,i-1)} + g_{(j,i)}v_{(j,i+1)} \\
\dot{v}_{(j,n_j)} &= -k_{(j,n_j)}v_{(j,n_j)} - g_{(j,n_j-1)}^{\mathsf{T}} v_{(j,n_j-1)}.
\end{aligned}$$

Denote $k_{(j,)} = \operatorname{diag}\{k_{(j,1)}, \ldots, k_{(j,n_j)}\}$ and $n_{(j,i:k)} = \sum_{l=i}^{k} n_{(j,l)}$. Define $G_{(j,)} \in \mathbb{R}^{n_{(j,1:n_j)} \times n_{(j,1:n_j)}}$, which is given by

$$G_{(j,)} = \begin{bmatrix} 0_{11} & \operatorname{diag}\{g_{(j,1)}, \ldots, g_{(j,n_j-1)}\} \\ 0_{21} & 0_{22} \end{bmatrix},$$

where $0_{11} \in \mathbb{R}^{n_{(j,1:(n_j-1))} \times n_{(j,1)}}$, $0_{21} \in \mathbb{R}^{n_{(j,n_j)} \times n_{(j,1)}}$, and $0_{22} \in \mathbb{R}^{n_{(j,n_j)} \times n_{(j,2:n_j)}}$ are zero matrices. Then, $\bar{G}_{(j,)} = \left(G_{(j,)} - G_{(j,)}^{\mathsf{T}}\right)$ is a *skew-symmetric* matrix. With these definitions, the expression above can be written in the compact form

$$\dot{v}_{(j,)} = -k_{(j,)}v_{(j,)} + \bar{G}_{(j,)}v_{(j,)} + \begin{bmatrix} \bar{u}_{(j,1)} \\ 0 \end{bmatrix}.$$

The Lyapunov function $V(v)$ can be rewritten as

$$V(v) = \frac{1}{2}\sum_{j=1}^{m} v_{(j,)}^{\mathsf{T}} v_{(j,)}.$$

Therefore the derivative is:

$$\begin{aligned}
\dot{V}(v) =& \sum_{j=1}^{m} v_{(j,)}^{\mathsf{T}} \dot{v}_{(j,)} \\
=& \sum_{j=1}^{m} -v_{(j,)}^{\mathsf{T}} k_{(j,)} v_{(j,)} + v_{(j,)}^{\mathsf{T}} \bar{G}_j v_{(j,)} + v_{(j,1)}^{\mathsf{T}} \bar{u}_{(j,1)} \\
=& \sum_{j=1}^{m} -v_{(j,)}^{\mathsf{T}} k_{(j,)} v_{(j,)} + v_{(j,1)}^{\mathsf{T}} \bar{u}_{(j,1)} \\
\le& - \bar{v}^{\mathsf{T}} \operatorname{diag}\{k_{(1,1)}, \ldots, k_{(m,1)}\}\bar{v} + \bar{v}^{\mathsf{T}}\bar{u} \\
\le& - \epsilon_b \bar{v}^{\mathsf{T}}\bar{v} + \bar{v}^{\mathsf{T}}\bar{u}.
\end{aligned}$$

■

Throughout the rest of the paper, we demonstrate how this result is applicable to the control of a quadrotor aircraft. From past experience, we know that our proposed framework is applicable to control of a fixed-wing aircraft. The dynamics of fixed-wing aircraft can be modeled by a 2-triangular system, such that the velocity control system is designed separately from the Velocity Flight Path and Velocity Heading Angle Control system [28]. We assert that Lemma 1 is applicable to the control of many other classes of systems, including robotic systems [5], ground vehicles [29] and certain classes of chemical processes [30]–[32]. Additionally, the m-triangular system formulation allows further model and control design simplification.

The main apparent limitation of our framework is related to the requirement that each matrix, $g_{(j,i)}$, has full row rank. This restriction implies that the system is at least *fully actuated* in the sense that the width of the state vectors, $x_{(j,i)} \in \mathbb{R}^{n_{(j,i)}}$, for a given j and $i \in \{1, \ldots, n_j\}$ can remain the same or contract in size as i decreases, so that $n_{(j,i)} \le n_{(j,i+1)}$ (recall, $u_j \in \mathbb{R}^{m_j}$, with $m_j = n_{(j,n_j+1)}$). This is why we suggest limited applicability to the chemical process control field. Recently, the process control community has been attempting to address control of underactuated systems through an emerging technique known as Interconnection Damping Assignent Passivity Based Control (IDA-PBC), which may be more suitable than our proposed framework [44]–[46].

Although many backstepping based control architectures have attempted to address the control of aircraft and ground vehicles, our observation is that these approaches tend to force the model into an awkward 1-triangular system formulation. We wrestled with this limitation for quite some time before realizing the m-triangular system formulation. A sketch for the proof of our aforementioned assertion will be made more evident as we recall the model for a quadrotor aircraft in Section VII and then provide our resulting realization, which describes the quadrotor aircraft as a 3-triangular system in Section VIII.

VII. Quadrotor Model

We briefly recall the quadrotor model presented in [27]. In [27], we presented, implemented, and verified a low complexity, high performance control architecture for the STARMAC quadrotor aircraft [47]. In order to derive a

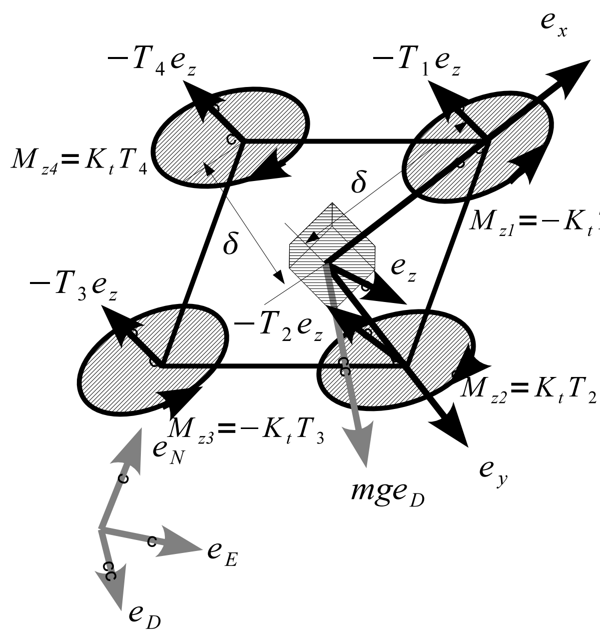

Fig. 2. UAV with depiction of inertial and body frames [27].

working model and control system for the STARMAC in a very short timeframe, we had to i) rely on the use of Euler angles in order to relate the aircraft's body frame to the inertial frame, and ii) rely on a constructive approach in which we approximated the system model as consisting of a cascade of four passive systems. The cascaded passive system model is not an unreasonable one since the inertial dynamics are indeed passive, as is the relationship between the control torque and the corresponding product of the inertia matrix and body angular velocities. Unfortunately, there still remains non-passive effects due to the use of Euler angles in relating the angular velocity to its corresponding attitude. These effects are most noticeable in low inertia quadrotor aircraft, such as the Hummingbird quadrotor aircraft [33], [34], and can be addressed with our proposed framework.

Let $\mathcal{I} = \{e_N, e_E, e_D\}$ (North-East-Down) denote the inertial frame, and $\mathcal{A} = \{e_x, e_y, e_z\}$ denote a frame rigidly attached to the aircraft, as depicted in Fig. 2. Let $\zeta = [\zeta_N, \zeta_E, \zeta_D]^\mathsf{T}$ denote inertial position, $v_I = [v_N, v_E, v_D]^\mathsf{T}$ denote the inertial velocity, and $\eta = [\phi, \theta, \psi]^\mathsf{T}$ denote the vector of Euler angles, in which ϕ is the roll, θ is the pitch, and ψ is the yaw. Let $R(\eta) \in \mathtt{SO}(3)$ be the orthogonal rotation matrix ($R^\mathsf{T} R = I$) that transforms the inertial coordinates to the body coordinates, as is the convention used in [48], [49]. The rotation matrix relates coordinates in the inertial frame, such as inertial angular velocity ω_I, to coordinates in the body frame, such as the angular velocity $\omega = [p, q, r]^\mathsf{T}$, as follows

$$\omega_I = R^\mathsf{T}(\eta)\omega.$$

The standard equations of motion are given by

$$\dot{\zeta} = v_I,$$
$$m\dot{v}_I = f_I = mge_D - TR^\mathsf{T}(\eta)e_z, \quad (8)$$
$$I_b\dot{\omega} = -\omega \times I_b\omega + \Gamma, \quad (9)$$
$$\dot{\eta} = J(\eta)\omega. \quad (10)$$

These kinematic equations result in a cascaded structure, where the inertial force (f_I) depends on the orientation, as described by the Euler angles, η. Specifically, using the shorthand notation $c_x = \cos x$ and $s_x = \sin x$, the rotation matrix $R(\eta)$ is related to the Euler angles as follows [48, Section 5.6.2]:

$$R(\eta) = \begin{bmatrix} c_\theta c_\psi & c_\theta s_\psi & -s_\theta \\ s_\phi s_\theta c_\psi - c_\phi s_\psi & s_\phi s_\theta s_\psi + c_\phi c_\psi & c_\theta s_\phi \\ c_\phi s_\theta c_\psi + s_\phi s_\psi & c_\phi s_\theta s_\psi - s_\phi c_\psi & c_\theta c_\phi . \end{bmatrix} \quad (11)$$

Also in (8), m is the mass of the quadrotor and $T \in \mathbb{R}$ is the sum of the thrust of the four rotors.

Next, $I_b = \mathrm{diag}\{I_{xx}, I_{yy}, I_{zz}\}$ in (9) is the inertia matrix with respect to the body frame, in which we neglect the non-diagonal terms due to the symmetry of the quadrotor aircraft (this is typically not the case for fixed-wing aircraft control). The cross product, denoted by the operator $(\omega\times)$, can be represented by the following skew-symmetric matrix $(-(\omega\times) = (\omega\times)^\mathsf{T})$:

$$(\omega\times) = \begin{bmatrix} 0 & -r & q \\ r & 0 & -p \\ -q & p & 0 \end{bmatrix}.$$

Finally, the body control torques are given by $\Gamma^\mathsf{T} = [\gamma_x, \gamma_y, \gamma_z]^\mathsf{T}$, where each control torque is applied about each corresponding principal axis, and positive torque follows the right hand rule.

In (10), $J(\eta)$ relates the body angular velocity, ω, to the rate of change of the Euler angles $\dot{\eta}$. The matrix $J(\eta)$ is the inverse of the Euler angle rates matrix $[E'_{123}(\eta)]^{-1}$ [48, Section 5.6.4], and is given by

$$J(\eta) = \begin{bmatrix} 1 & \sin\phi\tan\theta & \cos\phi\tan\theta \\ 0 & \cos\phi & -\sin\phi \\ 0 & \frac{\sin\phi}{\cos\theta} & \frac{\cos\phi}{\cos\theta} \end{bmatrix}. \quad (12)$$

Completing our discussion on the UAV dynamics, we note that the relationship between inertial acceleration, control thrusts, and the Euler angles is given by

$$m\dot{v}_I = \begin{bmatrix} 0 \\ 0 \\ mg \end{bmatrix} + f_{Ic}, \quad f_{Ic} = -T \begin{bmatrix} c_\phi s_\theta c_\psi + s_\phi s_\psi \\ c_\phi s_\theta s_\psi - s_\phi c_\psi \\ c_\theta c_\phi \end{bmatrix}, \quad (13)$$

where f_{Ic} denotes the inertial control force and $T = \sum_{i=1}^4 T_i$ is the total thrust applied by the four rotors. Ignoring blade flapping effects, the control torques Γ and total thrust T have the following relationship:

$$\begin{bmatrix} \gamma_x \\ \gamma_y \\ \gamma_z \\ T \end{bmatrix} = \begin{bmatrix} 0 & -\delta & 0 & \delta \\ \delta & 0 & -\delta & 0 \\ -K_t & K_t & -K_t & K_t \\ 1 & 1 & 1 & 1 \end{bmatrix} \begin{bmatrix} T_1 \\ T_2 \\ T_3 \\ T_4 \end{bmatrix}, \quad (14)$$

where δ is the distance from the center of gravity of the quadrotor for each rotor of the UAV along the x and y body frame axes, and K_t captures the relationship between the rotor velocity and the corresponding torques applied about the z-axis (see Fig. 2). It is assumed that $\delta K_t \neq 0$, so that the above matrix is invertible in order to relate the resulting thrust T and control torque Γ to the corresponding motor thrusts T_i.

Finally, there is a non-ideal lag between the resulting motor thrusts T_i and the desired thrust commands T_{id} associated with each rotor such that

$$T_i(s) = \frac{T_{id}(s)}{\tau s + 1}, \tag{15}$$

in which $\tau \approx .1$ seconds represents the thrust lag to each rotor, and cannot be neglected in designing the controller.

VIII. Quadrotor Model Realization

In this section, we describe the realization of the quadrotor model described in Section VII as a 3-triangular system. The first triangular system ($j = 1$) has system cascade length, $n_1 = 5$, and each of the states, $x_{(1,i)}$, have the same dimension, $n_{(1,i)} = 2$. The remaining two triangular systems ($j \in \{2,3\}$) are described using the scalar states $x_{(2,i)}$ and $x_{(3,i)}$ ($n_{(2,i)} = n_{(3,i)} = 1$), and have the same cascade length, $n_2 = n_3 = 3$. This implies that the remaining two models can be concatenated; however, it is much easier to understand these models when presented separately.

A. *Triangular subsystem* 1

The first triangular system relates the desired control torques applied about the x and y axes in the body coordinates to the inertial position of the quadrotor, in terms of north and east. The triangular system has a cascade length, $n_1 = 5$, where the input u_1 and the states $x_{(1,i)}$ are given by

$$u_1 = \begin{bmatrix}\gamma_{xd}\\ \gamma_{yd}\end{bmatrix}, \quad x_{(1,1)} = \begin{bmatrix}\zeta_N\\ \zeta_E\end{bmatrix}, \quad x_{(1,2)} = \begin{bmatrix}v_N\\ v_E\end{bmatrix},$$

$$x_{(1,3)} = \begin{bmatrix}\phi\\ \theta\end{bmatrix}, \quad x_{(1,4)} = \begin{bmatrix}p\\ q\end{bmatrix}, \quad x_{(1,5)} = \begin{bmatrix}\gamma_x\\ \gamma_y\end{bmatrix}.$$

Now, the input u_1 can be related to the state $x_{(1,5)}$ by assuming that γ_{xd} and γ_{yd} are related to the T_{id}, $i \in \{1,2,3,4\}$, in the same manner that γ_x and γ_y are related to the T_{id} in (14). Combining this with the non-ideal lag described in (15) yields

$$\begin{bmatrix}\dot{\gamma}_x\\ \dot{\gamma}_y\end{bmatrix} = -\frac{1}{\tau}\begin{bmatrix}\gamma_x\\ \gamma_y\end{bmatrix} + \frac{1}{\tau}\begin{bmatrix}\gamma_{xd}\\ \gamma_{yd}\end{bmatrix}.$$

Next, $x_{(1,5)}$ is related to $x_{(1,4)}$ through (9) by

$$\begin{bmatrix}\dot{p}\\ \dot{q}\end{bmatrix} = \begin{bmatrix}\frac{I_{yy}-I_{zz}}{I_{xx}} rq\\ \frac{I_{zz}-I_{xx}}{I_{yy}} rp\end{bmatrix} + \begin{bmatrix}\frac{1}{I_{xx}} & 0\\ 0 & \frac{1}{I_{yy}}\end{bmatrix}\begin{bmatrix}\gamma_x\\ \gamma_y\end{bmatrix}.$$

Using (10) and (12), we can relate $x_{(1,4)}$ to $x_{(1,3)}$ by

$$\begin{bmatrix}\dot{\phi}\\ \dot{\theta}\end{bmatrix} = \begin{bmatrix}r\cos\phi\tan\theta\\ -r\sin\phi\end{bmatrix} + \begin{bmatrix}1 & \sin\phi\tan\theta\\ 0 & \cos\phi\end{bmatrix}\begin{bmatrix}p\\ q\end{bmatrix}.$$

By making a small angle approximation ($\sin(\phi) = \phi$ and $\sin(\theta) = \theta$) in (13), we can relate $x_{(1,3)}$ to $x_{(1,2)}$ as follows:

$$\begin{bmatrix}\dot{v}_N\\ \dot{v}_E\end{bmatrix} = \left(-\frac{T}{m}\right)\begin{bmatrix}\sin\psi & \cos\phi\cos\psi\\ -\cos\psi & \cos\phi\sin\psi\end{bmatrix}\begin{bmatrix}\phi\\ \theta\end{bmatrix}.$$

Finally, $x_{(1,2)}$ is related to $x_{(1,1)}$ by

$$\begin{bmatrix}\dot{\zeta}_N\\ \dot{\zeta}_E\end{bmatrix} = \begin{bmatrix}v_N\\ v_E\end{bmatrix}.$$

In summary, the triangular system is parameterized by

$$f_{(1,1)} = 0, \qquad g_{(1,1)} = I,$$

$$f_{(1,2)} = 0, \qquad g_{(1,2)} = -\tfrac{T}{m}\begin{bmatrix}s_\psi & c_\phi c_\psi\\ -c_\psi & c_\phi s_\psi\end{bmatrix},$$

$$f_{(1,3)} = \begin{bmatrix}rc_\phi t_\theta\\ -rs_\phi\end{bmatrix}, \qquad g_{(1,3)} = \begin{bmatrix}1 & s_\phi t_\theta\\ 0 & c_\phi\end{bmatrix},$$

$$f_{(1,4)} = \begin{bmatrix}\frac{I_{yy}-I_{zz}}{I_{xx}} rq\\ \frac{I_{zz}-I_{xx}}{I_{yy}} rp\end{bmatrix}, \qquad g_{(1,4)} = \begin{bmatrix}\frac{1}{I_{xx}} & 0\\ 0 & \frac{1}{I_{yy}}\end{bmatrix},$$

$$f_{(1,5)} = -\tfrac{1}{\tau}\begin{bmatrix}\gamma_x\\ \gamma_y\end{bmatrix}, \qquad g_{(1,5)} = \tfrac{1}{\tau},$$

where we have used the shorthand notation $\tan x = t_x$, $\cos x = c_x$, and $\sin x = s_x$.

B. *Triangular Subsystem* 2

The second triangular system relates the desired total thrust T_d to the altitude of the quadrotor, $|\zeta_D|$. The triangular system has a cascade length, $n_2 = 3$, where the input u_2 and the states $x_{(2,i)}$ are given by

$$u_2 = T_d, \quad x_{(2,1)} = \zeta_D,$$
$$x_{(2,2)} = v_D, \quad x_{(2,3)} = T.$$

The altitude system dynamics can be represented by the following set of equations:

$$\dot{T} = -\frac{1}{\tau}T + \frac{1}{\tau}T_d,$$
$$\dot{v}_D = g - \frac{T}{m}\cos\phi\cos\theta,$$
$$\dot{\zeta}_D = v_D.$$

Thus, the triangular system is parameterized by

$$f_{(2,1)} = 0, \quad f_{(2,2)} = g, \quad f_{(2,3)} = -\tfrac{1}{\tau}T,$$

$$g_{(2,1)} = 1, \quad g_{(2,2)} = -\tfrac{c_\phi c_\theta}{m}, \quad g_{(2,3)} = \tfrac{1}{\tau}.$$

C. *Triangular subsystem* 3

The third triangular system relates the desired control torque applied about the z axis, γ_z, to the yaw angle of the quadrotor, ψ. The triangular system has a cascade length, $n_3 = 3$, where the input u_3 and the states $x_{(3,i)}$ are

$$u_3 = \gamma_{zd}, \quad x_{(3,1)} = \psi,$$
$$x_{(3,2)} = r, \quad x_{(3,3)} = \gamma_z.$$

The yaw system dynamics are described by the following set of equations:

$$\begin{aligned}\dot{\gamma}_z &= -\frac{1}{\tau}\gamma_z + \frac{1}{\tau}\gamma_{zd},\\ \dot{r} &= \frac{I_{xx}-I_{yy}}{I_{zz}}pq + \frac{1}{I_{zz}}\gamma_z,\\ \dot{\psi} &= q\phi + r.\end{aligned}$$

The triangular system is then parameterized by

$$f_{(3,1)}{=}q\phi,\quad f_{(3,2)}{=}\tfrac{I_{xx}-I_{yy}}{I_{zz}}pq,\quad f_{(3,3)}{=}{-}\tfrac{1}{\tau}\gamma_z,$$

$$g_{(3,1)}{=}1,\qquad g_{(3,2)}{=}\tfrac{1}{I_{zz}},\qquad g_{(3,3)}{=}\tfrac{1}{\tau}.$$

The advantage of our 3-Triangular System formulation for our quadrotor aircraft will be come readily apparent when comparing to the pioneering work of [50], [51] and quite recently the work of [52], [53]. There may be similar works derived from the pioneering work of [50]; however, to the best of our knowledge this represents state of the art for modeling quadrotor aircraft.

N.B. none of the aforementioned works had connected the pioneering work of [41], [54] as it related to a systematic procedure to derive an adaptive back-stepping control law which *could also account for actuator limitations such as saturation* while also allowing for the operating state-constraints to be addressed. So although Madani and Benalleque had begun to formulate a procedure to derive a backstepping control law based on a model similar to our $m-$Triangular system formulation it was not quite made precise and the resulting control laws which were derived were not done in a systematic or precise way. Interestingly [43] had noted the work of [51] yet was critical of their approximate approach in generating derivatives, which we concur. Typically the authors who resorted to techniques pioneered by [51] involved deriving auxiliary variables in order to obtain a $1-$Triangular system formulation.

IX. Networked Control of m-Triangular Systems

In this section, we shall demonstrate how to integrate a strictly-output passive discrete-time lag-compensator in order to implement a discrete-time inertial navigation system for a vehicle (which can be described as an m-Triangular System) which can also explicitly control a subset of the vehicles reference frame. As suggested earlier in our discussions, such vehicles include quadrotor, fixed-wing aircraft, ground vehicles and robotic systems. For the quadrotor example we have presented it shall be made clear that we can control the inertial position and its corresponding yaw over a discrete-time network which can be subject to time-varying delays and data loss. In order to do so, we shall build on our previous work in [24], [26] in order to derive a networked control architecture that is robust to time-varying delays and data loss. This networked control architecture is depicted in Fig. 3.

Assumption 1: Initially we shall *assume* i) that the continuous-time system $H_p : e_p \to y_p$ depicted in Fig. 3 is a *continuous-conic system* inside the sector $[a_p, b_p]$ as described in Section III (a slightly more general version of the continuous-conic-dissipative systems Definition 1); ii) that the discrete-time controller $H_c : e_c \to y_c$ depicted in Fig. 3 is a *discrete-conic-dissipative system* inside the sector $[a_c, b_c]$ (Definition 1); iii) the scattering gain ϵ satisfies the following bounds: a) $0 < \epsilon < \infty$, if $a_p \geq 0$ or b) $0 < \epsilon < -\frac{1}{2}\left(\frac{1}{a_p} + \frac{1}{b_p}\right)$ if $a_p < 0$; finally iv) the networked control system is constructed such that it is *well posed* [23].

We recall from [24] how the wave variable transform is implemented in terms of the positive real term ϵ. Specifically, the signals $u_p(t)$ and $v_p(t)$ ($u_c(j)$ and $v_c(j)$) depicted in Fig. 3 are continuous-time (discrete-time) *wave variables* in which their relationships are determined by a special type of *scattering transforms* [3] known as the *wave variable* transform [4]. Denote $I \in \mathbb{R}^{m\times m}$ as the identity matrix. When implementing the wave variable transformation the continuous time plant "outputs" $(u_p(t), y_{\mathsf{dc}}(t))$ are related to the corresponding "inputs" $(v_p(t), y_p(t))$ as follows (Fig. 3):

$$\begin{bmatrix} u_p(t) \\ y_{\mathsf{dc}}(t)\end{bmatrix} = \begin{bmatrix} -I & \sqrt{2\epsilon}I \\ -\sqrt{2\epsilon}I & \epsilon I\end{bmatrix}\begin{bmatrix} v_p(t) \\ y_p(t)\end{bmatrix} \tag{16}$$

Next, the discrete time controller "outputs" $(v_c(j), y_{\mathsf{dp}}(j))$ are related to the corresponding "inputs" $(u_c(j), y_c(j))$ as follows (Fig. 3):

$$\begin{bmatrix} v_c(j) \\ y_{\mathsf{dp}}(j)\end{bmatrix} = \begin{bmatrix} I & -\sqrt{\frac{2}{\epsilon}}I \\ \sqrt{\frac{2}{\epsilon}}I & -\frac{1}{\epsilon}I\end{bmatrix}\begin{bmatrix} u_c(j) \\ y_c(j)\end{bmatrix} \tag{17}$$

The wave variable from the plant, u_p, is sampled in the wave domain using the multi-rate passive sampler (PS) and passive hold (PH). The PS implements an *anti-aliasing filter* in order to remove band-limited noise without adversely affecting system stability. As a result this significantly allows one to improve system noise rejection performance [24]. Fig. 4 depicts the multi-rate PS and PH and their corresponding implementation equations. *N.B. In order to simplify discussion the multi-rate PS and PH are depicted for the scalar case.* However, *without any loss in generality*, the multi-rate PS and PH can be implemented in an identical manner as it relates to each individual element associated with its corresponding wave variables $u_p(t)$ and $v_c(j)$. With Assumption 1 and our multi-rate networked control architecture clearly presented we shall now present the following Lemma.

Lemma 2: Consider the digital control network depicted in Fig. 3 in which the plant, $H_p : e_p \to y_p$ and controller $H_c : e_c \to y_c$ satisfy the conditions of Assumption 1. If the plant and controller satisfy any one of the following combined set of conditions:

I. H_p is inside the sector $[0, b_p]$ and H_c is inside the sector $[0, b_c]$;
II. H_p is inside the sector $[0, \infty]$ and H_c is inside the sector $[a_c, b_c]$ such that $0 < a_c < b_c < \infty$ (or vice-versa);
III. H_p is inside the sector $[a_p, \infty]$ in which $a_p < 0$ and H_c is inside the sector $[a_c, b_c]$ such that $-\epsilon^2 a_p < a_c, b_c < -\frac{1}{a_p}$;

then the digital control network is L_2^m-stable.

Proof: (Sketch)

I. Lemma 2-I can be derived from [26, Corollary 1] in that H_p and H_c are strictly output passive systems.

II. Lemma 2-II can be derived from [24, Theorem 3] and [24, Corollary 1-1].

III. Lemma 2-III can be derived from [24, Theorem 3] and [24, Corollary 1-2].

■

It should be clear that there are a broad range of conditions on the discrete-time controllers which can be exploited in order to control a continuous-time plant which can be confined to a given sector. Lemma 2-I may appear to be a bit conservative at first; however, it essentially allows an engineer to integrate a discrete-time proportional-integral (PI) compensator in order to force all the outputs of the system to follow a desired discrete-time trajectory. A discrete-time PI (or lag) compensator can be designed to be inside the sector $[0, \infty]$ by applying either the *bilinear-transform* [25] or the *IPESH-Transform* [19, Definition 5] by diagonalizing the following analog controller $H_c(s) = K_P + K_I\left(\frac{s+\omega_I}{s}\right)$ as demonstrated in [55].

The aforementioned control law derived can be rendered strictly output passive by simply closing the loop in terms of the real coefficient $0 < \epsilon_b = \frac{1}{b_c} << 1$ such that it is constrained to be inside the sector $[0, b_c]$ as it approaches the ideal case $[0, \infty]$ in the limit as $\epsilon_b \to 0^+$ in which the strictly output passive controller is of the following form $H_{\mathsf{sop}}(s) = \frac{H_c(s)}{1+\epsilon_b H_c(s)}$. A more general *multivariable* discrete-time lag-type control law can be implemented as detailed in [26, Section D]. Finally, one side-effect of designing discrete-time controllers which are *passive* is that algebraic loops are introduced if they are implemented with the *wave variables*, however this can be handled precisely for the *LTI* case as detailed in [26, Section D].

This is why we added the condition *that the system is well posed* as our approach applies to non-linear systems. *A well posed* system is a system in which the instantaneous loop gains are less than one. This allows a feasible control law to be implemented. In practice we have developed techniques to run MATLABs *variable step solvers* in a real-time manner as it is related to control of a robotic arm. Therefore we believe that this is *an emerging area for research* to develop techniques to solve *well posed* algebraic loops for non-linear systems in a real-time manner. The other way we have been able to implement our proposed framework is to oversample the continuous-time system and introduce a single delay which allows us to achieve a well-posed system; however, we have to weaken our controller to be a discrete-time feed-forward lag type compensator derived from an analog controller of the following form $H_{\mathsf{ff-lag}}(s) = a_c + H_{\mathsf{sop}}(s)$ such that a_c and b_c satisfy the conditions in Lemma 2-III.

In order to present our final result as it relates to the control of m-Triangular Systems we need the a slightly less restrictive assumption.

Assumption 2: Assume we have a continuous-time system $H_{\mathsf{pm}} : u \to y = x$ which can be realized as an m-Triangular System as described in Section IV.

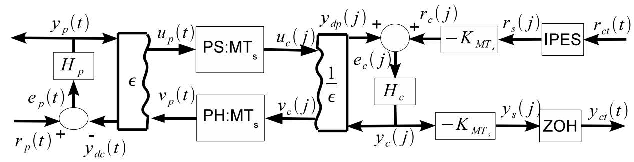

Fig. 3. Digital control network for continuous-time system [24].

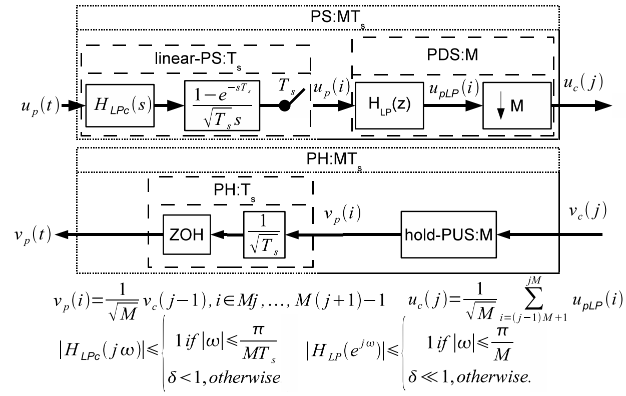

Fig. 4. Multi-rate passive sampler, passive hold [24].

Theorem 1: Consider the continuous-time system $H_{\mathsf{pm}} : u \to y = x$ as described by Assumption 2 which is subject to the back-stepping control framework described in Section V. The resulting closed-loop system $H_{\mathsf{cl}} : \bar{u} \to \bar{v}$ is then integrated into the digital control network depicted in Fig. 3 such that plant $H_p = H_{\mathsf{cl}}$ in which $e_p = \bar{u}$ and $y_p = \bar{v}$. Therefore, if the digital controller H_c is inside the sector $[0, b_c]$ then the resulting digital control network is L_2^m-stable.

Proof: From Lemma 1 we know that the back-stepping control framework allows for the plant $H_{\mathsf{pm}} : u \to y = x$ to be rendered strictly output passive such that $H_p : e_p \to y_p$ is inside the sector $[0, b_p]$. Therefore from Lemma 2-I the resulting digital control network is L_2^m-stable. ■

It is left as an exercise for the reader to show that the quadrotor aircraft described in Section VII and Section VIII can be integrated into our proposed framework such that an overall L_2^m-stable network can be constructed. It remains an *unproven assertion* that the backstepping framework can be extended to continuous-time backstepping control frameworks in particular as it relates to *multiparameter systems* in order to derive much stronger stability results for the non-scalar case [43].

X. Remote Navigation of Quadrotor Aircraft

Throughout the years we have constructed and tested high-performance controllers for quadrotor aircraft [27] and fixed-wing aircraft [28]. In [27] we constructed low-complexity, high-performance controllers by simply approximating the quadrotor aircraft as a cascade of four passive systems, a special subclass of 1-Triangular Systems. We relied on [27, Corollary 2] to justify our initial designs in that it provided a sufficient condition for the limits of each nested feedback loop gains to satisfy L_2^m-stability. In [28] we discovered that unlike a quadrotor aircraft, a fixed-wing aircraft depends on the wind velocity vector which results in system model formulation which can not be reasonably approximated as a cascade of passive systems. We, initially relied on the 1-Triangular system formulation and chose two simplified non-adaptive backstepping control laws inspired from the earlier work of [41] in which the 1-Triangular system model was an improvement but not precisely correct. As we have demonstrated, a quadrotor aircraft can be more appropriately described by a 3-Triangular Systems model. In addition we assert that at least a 2-Triangular Systems model is necessary to design a high performance discrete-time aircraft navigation system.

Therefore, it is a straightforward exercise to develop an advanced simulation involving a ground control station providing inertial navigation for both *unmanned* quadrotor aircraft and fixed-wing aircraft in a shared NEXTGEN airspace [56]. The quadrotor aircraft as described in Section VII and modeled in Section VIII can be rendered to be strictly output passive using the backstepping control framework described in Section V. Finally, the aircraft and its corresponding backstepping controller can be integrated into the advanced digital control framework depicted in Fig. 3 in which the ground control station can consist of a dedicated lag-digital controller H_c to maintain a an appropriately scaled desired continuous-time trajectory $r_{ct}(t)$ which can be pre-computed by the non-causal formulation of the inner-product equivalent sampler (IPES) [26, Section E]. The IPES is primarily used for analysis in order to satisfy L_2^m-stability.

It is quite difficult to precisely guarantee continuous-time stability of non-linear systems which are subject to discrete-time control. Therefore, we encourage the engineer not to get overly distracted by the formulation of the IPES and to focus on understanding how the discrete-time $r_c(j)$ references relate to the corresponding outputs $y_p(t)$. The engineer should simply study [26, Lemma 4] in order to understand how $r_c(j)$ relates to $y_p(t)$ in the limit as the steady-state controller gain $k_c \to \infty$ ($H_{\mathsf{sop}}(s) \approx H_c(s)$ as $\epsilon_b \to 0^+$).

Finally we would like to emphasize that the multi-rate passive sampler and passive hold devices will allow for high-performance discrete-time navigation of the aircraft. Precisely these devices can be engineered to adapt their data-rates in order to match channel capacity. In addition if bursty-like communication properties arise due to poor weather conditions, then system stability can still be guaranteed in spite of random time-varying delays and data loss.

XI. Conclusion

In summary:

1) In Section IV we presented a *new formulation* to model non-linear systems which are affine in their input which we call m-Triangular Systems.
2) Using the m-Triangular Systems model, in Section V we presented a backstepping control framework which can render an m-Triangular System to be strictly output passive as stated in Lemma 1 and proven in Section VI.
3) In Section VIII we demonstrated how a quadrotor aircraft (Section VII) can be modeled as a 3-Triangular System.
4) In Section IX we presented our advanced networked digital control framework as depicted in Fig. 3. Lemma 2 presents a set of three unique conditions, each of which can be independently applied to a *continuous-conic* system which is inside the sector $[a_p, b_p]$ and its corresponding digital controller which is inside the sector $[a_c, b_c]$ such that the digital control framework is L_2^m-stable.
5) Finally, we present Theorem 1 in order to demonstrate how Lemma 1 and Lemma 2 can be used to show how an m-Triangular System can be rendered strictly output passive and integrated into our advanced networked digital control framework such that the overall system is L_2^m-stable.

We left it as an exercise for the reader to prove that a quadrotor aerial vehicle, modeled as a 3-Triangular System can be integrated into our framework such that a *digital lag compensator* could be used to maintain a desired course trajectory for an unmanned aerial vehicle subject to *actuator limitations such as actuator saturation* in a L_2^m-stable manner. Furthermore, in Section X we described how the inertial position of a quadrotor aircraft can be maintained by a ground-control station over a *wireless communication network* in a L_2^m-stable manner *in spite of random time-varying delays and data-loss*. It is left as an assertion that this overall framework is applicable to the control of many other classes of systems, including robotic systems [5], ground vehicles [29] and certain classes of chemical processes [30]–[32].

XII. Acknowledgements

We would like to acknowledge Gabor Karsai who helped us provide this work in a timely and professional manner. In addition we would like to acknowledge Xenofon D. Koutsoukos, Janos Sztipanovits, Panos Antsaklis and Jay Farrell for thoughtful discussions on this problem.

References

[1] A. Shajii, N. Kottenstette, and J. Ambrosina, "Apparatus and method for mass flow controller with network access to diagnostics," U.S. Patent 6 810 308, 2004, u.S. Patent #6810308.

[2] F. Lian, J. Moyne, and D. Tilbury, "Performance evaluation of control networks: Ethernet, ControlNet, and DeviceNet," *Control Systems Magazine, IEEE*, vol. 21, no. 1, pp. 66–83, 2001.

[3] R. J. Anderson and M. W. Spong, "Asymptotic stability for force reflecting teleoperators with time delay," *The International Journal of Robotics Research*, vol. 11, no. 2, pp. 135–149, 1992.

[4] G. Niemeyer and J.-J. E. Slotine, "Towards force-reflecting teleoperation over the internet," *Proceedings - IEEE International Conference on Robotics and Automation*, vol. 3, pp. 1909 – 1915, 1998.

[5] N. Chopra, P. Berestesky, and M. Spong, "Bilateral teleoperation over unreliable communication networks," *IEEE Transactions on Control Systems Technology*, vol. 16, no. 2, pp. 304–313, 2008.

[6] S. Hirche and M. Buss, "Transparent Data Reduction in Networked Telepresence and Teleaction Systems. Part II: Time-Delayed Communication," *Presence: Teleoperators and Virtual Environments*, vol. 16, no. 5, pp. 532–542, 2007.

[7] M. Kuschel, P. Kremer, and M. Buss, "Passive haptic data-compression methods with perceptual coding for bilateral presence systems," *IEEE Transactions on Systems, Man and Cybernetics, Part A: Systems and Humans*, vol. 39, no. 6, pp. 1142 – 1151, Nov. 2009.

[8] N. Kottenstette, "Control of passive plants with memoryless nonlinearitites over wireless networks," Ph.D. dissertation, University of Notre Dame, August 2007.

[9] N. Kottenstette and P. J. Antsaklis, "Wireless digital control of continuous passive plants over token ring networks," *International Journal of Robust and Nonlinear Control*, 2008.

[10] S. Stramigioli, C. Secchi, A. J. van der Schaft, and C. Fantuzzi, "Sampled data systems passivity and discrete port-hamiltonian systems," *IEEE Transactions on Robotics*, vol. 21, no. 4, pp. 574 – 587, 2005.

[11] J.-H. Ryu, D.-S. Kwon, and B. Hannaford, "Stable teleoperation with time-domain passivity control," *IEEE Transactions on Robotics and Automation*, vol. 20, no. 2, pp. 365 – 73, 2004/04/. [Online]. Available: http://dx.doi.org/10.1109/TRA.2004.824689

[12] A. van der Schaft and B. Maschke, "The Hamiltonian formulation of energy conserving physical systems with external ports," *AEU. Archiv fur Elektronik und Ubertragungstechnik*, vol. 49, no. 5-6, pp. 362–371, 1995.

[13] C. Secchi, S. Stramigioli, and C. Fantuzzi, *Control of interactive robotic interfaces: A port-Hamiltonian approach*. Springer Verlag, 2007.

[14] J. Filippo, M. Delgado, C. Brie, and H. Paynter, "A survey of bond graphs: Theory, applications and programs," *Journal of the Franklin Institute*, vol. 328, no. 5-6, pp. 565–606, 1991.

[15] P. Gawthrop and G. Bevan, "Bond-graph modeling," *Control Systems Magazine, IEEE*, vol. 27, no. 2, pp. 24–45, 2007.

[16] N. Kottenstette and P. Antsaklis, "Stable digital control networks for continuous passive plants subject to delays and data dropouts," *46th IEEE Conference on Decision and Control*, pp. 4433–4440, 2007.

[17] R. Costa-Castello and E. Fossas, "On preserving passivity in sampled-data linear systems," *2006 American Control Conference (IEEE Cat. No. 06CH37776C)*, pp. 6 pp. –, 2006.

[18] ——, "On preserving passivity in sampled-data linear systems," *European Journal of Control*, vol. 13, no. 6, pp. 583 – 590, 2007. [Online]. Available: http://dx.doi.org/10.3166/ejc.13.583-590

[19] N. Kottenstette, J. Hall, X. Koutsoukos, P. Antsaklis, and J. Sztipanovits, "Digital control of multiple discrete passive plants over networks," *International Journal of Systems, Control and Communications (IJSCC)*, no. Special Issue on Progress in Networked Control Systems, 2011, to Appear.

[20] N. Kottenstette and P. Antsaklis, "Digital control networks for continuous passive plants which maintain stability using cooperative schedulers," University of Notre Dame, Tech. Rep. isis-2007-002, March 2007, revised 1/2010. [Online]. Available: http://www.nd.edu/~isis/techreports/isis-2007-002-updated.pdf

[21] ——, "Wireless Control of Passive Systems Subject to Actuator Constraints," *47th IEEE Conference on Decision and Control, 2008. CDC 2008*, pp. 2979–2984, 2008.

[22] G. Zames, "On the input-output stability of time-varying nonlinear feedback systems. i. conditions derived using concepts of loop gain, conicity and positivity," *IEEE Transactions on Automatic Control*, vol. AC-11, no. 2, pp. 228 – 238, 1966.

[23] J. C. Willems, *The Analysis of Feedback Systems*. Cambridge, MA, USA: MIT Press, 1971.

[24] N. Kottenstette, H. LeBlanc, E. Eyisi, and X. Koutsoukos, "Multi-rate networked control of conic (dissipative) systems," in *Proceedings of the American Control Conference*, June 2011, (to appear), see technical report at. [Online]. Available: http://www.isis.vanderbilt.edu/sites/default/files/tr_quantization_final_ref.pdf

[25] L. Hitz and B. Anderson, "Discrete positive-real functions and their application to system stability," *Proc. IEE*, vol. 116, no. 1, pp. 153–155, 1969.

[26] N. Kottenstette, J. Hall, X. Koutsoukos, J. Sztipanovits, and P. Antsaklis, "Passivity-Based Design of Wireless Networked Control Systems Subject to Time-Varying Delays," *Provisionally Accepted to IEEE Transactions on Control Systems Technology*, pp. 2–17, 2011. [Online]. Available: http://www.isis.vanderbilt.edu/sites/default/files/passivity_isis_tr_08-904_revised_2_15_11.pdf

[27] N. Kottenstette and J. Porter, "Digital passive attitude and altitude control schemes for quadrotor aircraft," in *IEEE International Conference on Control and Automation (ICCA 2009)*, 2009, pp. 1761–1768, please refer to updated technical-report. [Online]. Available: http://www.isis.vanderbilt.edu/node/4051

[28] N. Kottenstette, "Constructive non-linear control design with applications to quad-rotor and fixed-wing aircraft," Institute for Software Integrated Systems, Vanderbilt University, Nashville, TN, Tech. Rep., January 2010. [Online]. Available: http://www.isis.vanderbilt.edu/node/4144

[29] V. Djapic, J. Farrell, and W. Dong, "Land vehicle control using a command filtered backstepping approach," in *Proceedings of the American Control Conference*, 2008, pp. 2461–2466.

[30] J. Bao, P. L. Lee, F. Wangc, W. Zhou, and Y. Samyudia, "A new approach to decentralised process control using passivity and sector stability conditions," *Chemical Engineering Communications*, vol. 182, no. 1, pp. 213–237, 2000.

[31] B. E. Ydstie, "Passivity based control via the second law," *Computers & Chemical Engineering*, vol. 26, no. 7-8, pp. 1037–1048, 2002.

[32] K. Jillson and B. Erik Ydstie, "Process networks with decentralized inventory and flow control," *Journal of Process Control*, vol. 17, no. 5, pp. 399–413, 2007.

[33] *AscTec Hummingbird with AutoPilot User's Manual*. [Online]. Available: http://www.asctec.de

[34] N. Michael, D. Mellinger, Q. Lindsey, and V. Kumar, "The GRASP multiple Micro-UAV testbed," *Robotics & Automation Magazine, IEEE*, vol. 17, no. 3, pp. 56–65, 2010.

[35] D. J. Hill, "Dissipative nonlinear systems: Basic properties and stability analysis," *Proceedings of the 31st IEEE Conference on Decision and Control*, pp. 3259–3264, 1992.

[36] D. J. Hill and P. J. Moylan, "The stability of nonlinear dissipative systems," *IEEE Transactions on Automatic Control*, vol. AC-21, no. 5, pp. 708 – 11, 1976.

[37] ——, "Stability results for nonlinear feedback systems," *Automatica*, vol. 13, pp. 377–382, 1977.

[38] G. C. Goodwin and K. S. Sin, *Adaptive Filtering Prediction and Control*. Englewood Cliffs, New Jersey 07632: Prentice-Hall, Inc., 1984.

[39] W. M. Haddad and V. S. Chellaboina, *Nonlinear Dynamical Systems and Control: A Lyapunov-Based Approach*. Princeton, New Jersey, USA: Princeton University Press, 2008.

[40] N. Kottenstette and J. Porter, "Digital passive attitude and altitude control schemes for quadrotor aircraft," Dec. 2009, pp. 1761 –1768.

[41] J. A. Farrell, M. Sharma, and M. Polycarpou, "Backstepping-based flight control with adaptive function approximation," *Journal of Guidance, Control, and Dynamics*, vol. 28, no. 6, pp. 1089–1102, 2005.

[42] M. Polycarpou, J. Farrell, and M. Sharma, "On-line approximation control of uncertain nonlinear systems: issues with control input saturation," in *Proceedings of the American Control Conference*, vol. 1, June 2003, pp. 543 – 548.

[43] J. A. Farrell, M. Polycarpou, M. Sharma, and W. Dong, "Command filtered backstepping," *IEEE Transactions on Automatic Control*, vol. 54, no. 6, pp. 1391 –1395, 6 2009.

[44] R. Ortega, A. Van Der Schaft, B. Maschke, and G. Escobar, "Interconnection and damping assignment passivity-based control of port-controlled Hamiltonian systems," *Automatica*, vol. 38, no. 4, pp. 585–596, 2002.

[45] H. Ramírez, D. Sbarbaro, and R. Ortega, "On the control of non-linear processes: An IDA-PBC approach," *Journal of Process Control*, vol. 19, no. 3, pp. 405–414, 2009.

[46] F. Dörfler, J. Johnsen, and F. Allgöwer, "An introduction to interconnection and damping assignment passivity-based control in process engineering," *Journal of Process Control*, 2009.

[47] G. M. Hoffmann, H. Huang, S. L. Waslander, and C. J. Tomlin, "Quadrotor helicopter flight dynamics and control: Theory and experiment," *Collection of Technical Papers - AIAA Guidance, Navigation, and Control Conference 2007*, vol. 2, pp. 1670 – 1689, 2007.

[48] J. Diebel, "Representing Attitude: Euler Angles, Unit Quaternions, and Rotation Vectors," Technical report, Stanford University, California, USA, Tech. Rep., 2006.

[49] L. Mangiacasale, *Flight Mechanics of a [mu]-airplane: With a Matlab Simulink Helper*. Edizioni Libreria CLUP, 1998.

[50] T. Madani and A. Benallegue, "Backstepping control for a quadrotor helicopter," in *International Conference on Intelligent Robots and Systems (2006 IEEE/RSJ)*, 2006, pp. 3255–3260.

[51] ——, "Control of a quadrotor mini-helicopter via full state backstepping technique," in 45th *IEEE Conference on Decision and Control (CDC 2006)*, 2006, pp. 1515–1520.

[52] M. Huang, B. Xian, C. Diao, K. Yang, and Y. Feng, "Adaptive tracking control of underactuated quadrotor unmanned aerial vehicles via backstepping," in *American Control Conference (ACC 2010)*, 2010, pp. 2076–2081.

[53] C. Nicol, C. Macnab, and A. Ramirez-Serrano, "Robust adaptive control of a quadrotor helicopter," *Mechatronics*, 2011.

[54] J. Farrell, M. Polycarpou, and M. Sharma, "On-line approximation based control of uncertain nonlinear systems with magnitude, rate and bandwidth constraints on the states and actuators," *Proceedings of the 2004 American Control Conference*, pp. 2557–2562, 2004.

[55] Y. Fu, N. Kottenstette, Y. Chen, C. Lu, X. Koutsoukos, and H. Wang, "Feedback thermal control for real-time systems," in *16*$^{\text{th}}$ *IEEE Real-Time and Embedded Technology and Applications Symposium (RTAS)*, 2010, pp. 111–120. [Online]. Available: http://cse.wustl.edu/Research/Lists/Technical%20Reports/Attachments/867/tcub1.pdf

[56] T. Prevot, J. Homola, and J. Mercer, "Human-in-the-loop evaluation of ground-based automated separation assurance for NEXTGEN," *Anchorage, Alaska: AIAA-ATIO-2008-8885*, 2008.